ISSN 2176-5480

22nd International Congress of Mechanical Engineering (COBEM 2013)
November 3-7, 2013, Ribeirão Preto, SP, Brazil
Copyright © 2013 by ABCM

AISI 420 MARTENSITIC STAINLESS STEEL LOW-TEMPERATURE PLASMA ASSISTED CARBURIZING, NITRIDING AND NITROCARBURIZING

Cristiano José Scheuer[a,b]**,** cristiano.scheuer@ufsm.br
Adriano David dos Anjos[a], adriano_david_anjos@hotmail.com
Rodrigo Perito Cardoso[a]**,** rodrigo.perito@ufpr.br
Valdir Bólico Araujo[b]**,** bolico@ctism.ufsm.br
Sílvio Francisco Brunatto[a]**,** brunatto@ufpr.br

[a] *Grupo de Tecnologia de Fabricação Assistida por Plasma e Metalurgia do Pó* (Plasma Assisted Manufacturing Technology & Powder Metallurgy Group) – *Departamento de Engenharia Mecânica, Universidade Federal do Paraná, 81531-990, Curitiba, PR, Brazil.*

[b] *Colégio Técnico Industrial de Santa Maria (CTISM), Universidade Federal de Santa Maria, 97105-900, Santa Maria, RS, Brazil.*

Abstract. *AISI 420 martensitic stainless steel samples were plasma carburized, nitrided and nitrocarburized at low temperatures. Treatments were carried out in pulsed DC glow discharge applying the following process parameters: 700 V peak voltage, 400 Pa pressure, 1.66 × 10^{-6} Nm^3 s^{-1} gas flow rate, at temperatures of 350, 400 and 450°C for a treatment time of 8 h. Gas mixtures composed of 99.5% (80% H_2 + 20% Ar) + 0.5% CH_4, 70% N_2 + 20% H_2 + 10% Ar and 71% N_2 + 18% H_2 + 10% Ar + 1% CH_4 were employed for the carburizing, nitriding and nitrocarburizing treatments, respectively. The metallurgical characterization of the untreated and plasma treated sample surfaces was performed using different techniques, aiming to compare the obtained phase constituents (XRD), microstructures (optical microscopy) and hardness (surface microhardness and microhardness profile). Results show significant increase of the surface hardness for all the studied samples. Precipitation-free treated layers were obtained for the lowest studied treatment temperature. The estimated activation energy for treated layer growth presents distinct values for the different types of treatments. Finally, for high temperature treatments, the carbide/nitride formation consumes significant amount of carbon/nitrogen, thus reducing the concentration gradient of these elements in solid solution, slowing down its diffusion depths in the martensite lattice.*

Keywords: *plasma carburizing, plasma nitriding, plasma nitrocarburizing, AISI 420 martensitic stainless steel, carbon expanded martensite, nitrogen expanded martensite.*

1. INTRODUCTION

Thermochemical treatments like plasma assisted nitriding, nitrocarburizing and carburizing have been widely used in industrial segments aiming to improve the surface properties of low alloy steels and tool steels [1]. The great potential of plasma assisted techniques is due to the achievement of excellent surface properties through their application in most engineering materials. In the case of stainless steel, an excellent combination between tribological properties and corrosion resistance can be obtained even for low temperatures or short treatment times [2-7]. When these treatments are performed at high temperatures (usually above 450°C), chromium nitride/carbide precipitation occurs, leading to a reduction of the material corrosion resistance [8,9].

The research interest on low-temperature thermochemical treatments for stainless steels has been strongly increased from the 1980s, since the nitrogen-expanded austenite phase (γ_N or *S* phase) was achieved [1, 2]. As a main result of this goal, many plasma assisted processes have been successfully tested and applied for stainless steels, making possible to achieve wear and corrosion resistance improvements for the treated materials [1]. In addition, as previously reported by Scheuer *et al.* [10], and guided by promising results, different plasma assisted techniques comprising DC plasma, RF plasma, plasma-based low-energy ion implantation, and plasma immersion ion implantation have been also tested for stainless steels. The great amount of works published on stainless steels' pulsed DC plasma treatments show the true technological potential of this technique. Considering the martensitic stainless steels, many works have been found reporting the use of low-temperature DC plasma assisted nitriding [1,4,11-17], nitrocarburizing [1,17-21] and carburizing [1,10, 22,23].

It is worth to emphasize a Sun and Bell [1] comparative study of low-temperature plasma nitriding, nitrocarburizing and carburizing, which was performed in martensitic stainless steel substrates, for a single experimental condition (450ºC treatment temperature and 20 h treatment time). In that work, it was stated that plasma carburizing did not produce significant hardening effect in treated surfaces of AISI 410 stainless steel samples. Contrarily, it was shown by Scheuer *et al*. [10,22,23] that an adequate choice of carburizing treatment parameters can lead to interesting results for

AISI 420 martensitic stainless steel substrates. Based on this new perspective, the aim of the present study is to compare the effects of the low-temperature and short-time DC plasma assisted nitriding, nitrocarburizing and carburizing treatments on the metallurgical characteristics of AISI 420 martensitic stainless steel substrates.

2. EXPERIMENTAL PROCEDURE

Cylindrical samples of 10 mm in height and 9.5 mm in diameter were cut from AISI 420 martensitic stainless steel commercial bar. They were oil quenched from 1050°C, after 0.5 h at the austenitizing temperature. The sample hardness in the as-quenched condition was 510 ± 10 $HV_{0.3}$. After heat treatment, samples were ground using SiC sandpaper ranging from 100 to 1200 grade and polished using 1 μm Al_2O_3 abrasive suspension. Finally, samples were alcohol cleaned in ultrasonic bath and then introduced into the discharge chamber.

The plasma treatment procedure was divided in two steps: a) aiming to remove the native oxide layer from sample surface, the specimens were sputter-cleaned by means of a 700 V peak voltage glow discharge, in a gas mixture of 80% H_2 + 20% Ar, under a pressure of 400 Pa, at 300°C, during 0.5 h; and, after cleanness, b) the specimens were plasma carburized, nitrided and nitrocarburized, in a gas mixture of 99.5% (80% H_2 + 20% Ar) + 0.5% CH_4, 70% N_2 + 20% H_2 + 10% Ar and 71% N_2 + 18% H_2 + 10% Ar + 1% CH_4, in volume, respectively. The total gas flow rate and pressure were kept unaltered for 1.66×10^{-6} $Nm^3\ s^{-1}$ and 400 Pa, respectively. Treatments were performed at 350, 400 and 450°C, for a single treatment time of 8 h. The plasma apparatus is constituted of a 4.16 kHz square-wave pulsed DC power supply, and a stainless steel cylindrical vacuum chamber of 350 mm in diameter and 380 mm high, attached to steel plates sealed with silicone o-rings at both the ends. The system was pumped down to a residual pressure on the order of 3 Pa using a double stage mechanical vacuum pump. The gas mixture and flow rate of H_2, N_2, Ar and CH_4 were adjusted by four mass flow controllers, three of 8.33×10^{-6} Nm^3s^{-1} and one of 8.33×10^{-8} Nm^3s^{-1}, respectively.

Samples were placed on the cathode of the discharge, which was negatively biased at 700 V. The samples' heating was a result of ions and fast neutrals species bombardment. The mean power transferred to the plasma, and consequently the treatment temperature, was adjusted by varying the switched-on time (t_{ON}) of the pulsed voltage. The temperature was measured by means of a chromel-alumel thermocouple (K-type of 1.5 mm diameter) inserted 8 mm depth into the sample holder. The pressure in the vacuum chamber was measured by a capacitive manometer of 1.33×10^4 Pa in full-scale operation and adjusted by a manual valve.

For microstructure analysis purpose, samples were prepared by conventional metallographic procedure. After polishing, the cross-sectioned samples were etched using Marble's reagent (4 g of Cu_4SO_4 + 20 ml of HCl + 20 ml of H_2O). Samples were examined using an Optical Microscope (Olympus BX51M). The identification of the phases present in the treated layers was carried out by X-ray diffractometry (XRD), using a Shimadzu XDR 7000 X-ray diffractometer with a Cu $K\alpha$ X-ray tube in the Bragg-Brentano configuration. Microhardness profiles were performed by using a Shimadzu Micro Hardness Tester HMV-2T, applying a load of 10 gf and a peak-load contact of 15 s. The points presented in each profile were obtained from a mean of five measurements. The diffusion layer depth was determined via microhardness profiles, considering that it occurs up to the depth for which the hardness becomes constant (agreeing with the hardness of the substrate bulk). It is to be noted that the bulk hardness varies according to the treatment temperature, since the tempering of the samples was performed simultaneously to the thermochemical treatment. Surface hardness measurements were performed employing the same equipment, applying load of 300 gf and peak-load contact of 15 s. In this case, the presented surface hardness values are also a mean of five measurements.

3. RESULTS AND DISCUSSION

Figure 1 shows the cross-section micrographs obtained after plasma carburizing, nitrocarburizing and nitriding treatments. It is found for the different plasma assisted treatments that the treated layer thickness increases as the treatment temperature increase. It can be clearly seen that the carburized layer thickness is smaller than the nitrocarburized one, which is smaller than the nitrided one, for all studied conditions (see Table 1). It is also observed the occurrence of sensitization for samples nitrided and nitrocarburized at 400 and 450°C, agreeing with the XRD data presented in Figure 3. It is to be noted that the white aspect of the 350°C treated layers is strongly changed by the black spots presence in the layers obtained at 400 and 450°C, supposedly indicating the CrN or Cr_xC_y formation.

Table 1. Layer thickness for different plasma treatment conditions.

Treatment temperature (°C)	Layer thickness (μm)		
	Carburized	Nitrocarburized	Nitrided
350	1.5 ± 0.2	4.6 ± 0.8	9.8 ± 1.1
400	1.8 ± 0.2	17.5 ± 0.4	21.2 ± 0.8
450	2.2 ± 0.2	45.8 ± 0.9	60.7 ± 0.7

ISSN 2176-5480

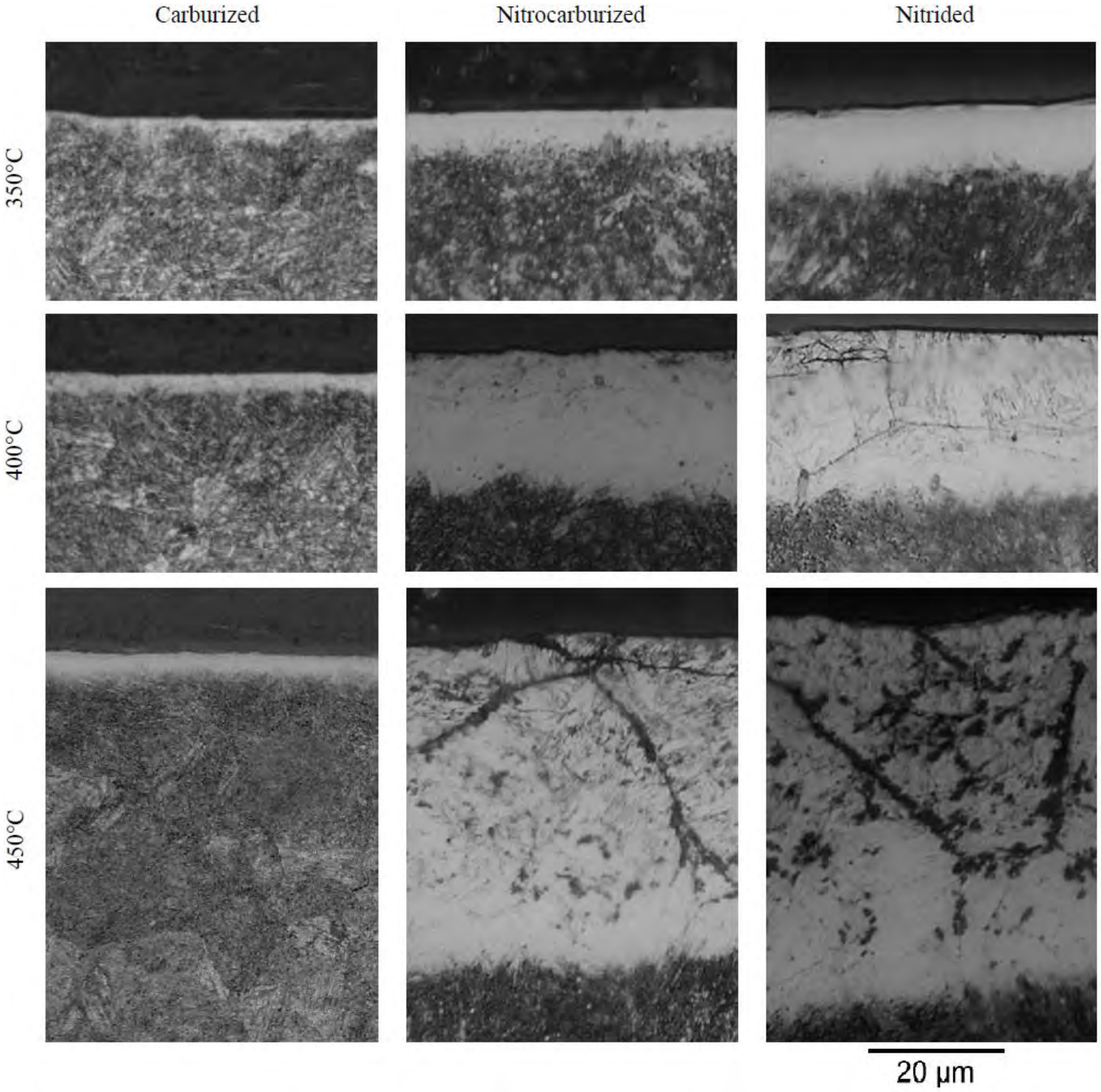

Figure 1. Cross-section microstructure of low-temperature plasma treated AISI 420 martensitic stainless steel. Treatments carried out for 8 h, at a flow rate of 1.67×10^{-6} Nm^3 s^{-1}, applied voltage of 700 V, and pressure of 400 Pa.

In Figure 2 the Arrhenius plot of the layer thickness is presented. If considered that the limiting process for treated layer growth is the nitrogen/carbon diffusion and that the layer thickness is proportional to the square root of the treatment time and diffusion coefficient (in agreement with the Arrhenius law), by linearization one can obtain the activation energy for diffusion of nitrogen and/or carbon during the plasma assisted process. From the Arrhenius plot, it is found that the nitrocarburizing treatment has the highest activation energy (173 $kJmol^{-1}$), followed by nitriding treatment (136 $kJmol^{-1}$) and the carburizing process presenting the lowest value (29 $kJmol^{-1}$). According to Pinedo and Monteiro [26], the activation energy for plasma nitrided AISI 420 steel at 480 to 560°C, and 4 h is 125.13 $kJmol^{-1}$. Amaral [25] show that the activation energy for low temperature dc-plasma nitriding (300 to 500°C and 4 h) of as-quenched, tempered and annealed AISI 420 steel is 60.0, 92.0 and 164.0 $kJmol^{-1}$, respectively. Furthermore, according to Scheuer *et al.* [24], the activation energy for plasma nitrocarburized AISI 420 steel at low-temperature, and 4 h treatment time is 84 $kJmol^{-1}$. However, at these treatment conditions, the volume diffusion of nitrogen and/or carbon through the modified layer is the main occurring phenomenon, without nitride/carbide precipitation, affecting significantly the diffusion process. Comparing to the previously presented results [24,25], the occurrence of nitride/carbide precipitation under the conditions employed in this work is the reason to the highest obtained values for the activation energy. For long-term and high-temperature plasma treatments, where nitride/carbide precipitation is ready to occur, the nitrided/nitrocarburized layer growth is affected by the precipitation effect, affecting the value of the estimated activation energy [26].

ISSN 2176-5480

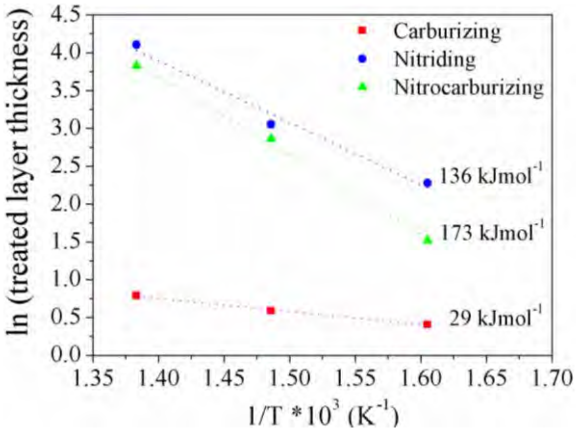

Figure 2. Arrhenius plot of the layer thickness for the low-temperature plasma treated surfaces. Treatments carried out for 8 h, at a flow rate of 1.67×10^{-6} Nm^3 s^{-1}, applied voltage of 700 V, and pressure of 400 Pa.

X-ray diffraction patterns of untreated (as-quenched) and plasma nitrided, carburized and nitrocarburized samples, treated at different temperatures are presented in Figure 3 (a,b,c). The as-quenched sample presents a peak related to the martensite phase (α′) in accordance with Xi *et al.* [13-15]. For low-temperature plasma nitrided samples (350°C) the phases are mainly ε-$Fe_{2\text{-}3}N$ and α'_N. For higher temperature nitriding conditions (400 and 450°C), CrN precipitation is also evidenced, confirming the occurrence of sensitization, as indicated in Figure 1. Further, for the carburized samples, it is observed the occurrence of Fe_3C and α'_C phases, and no precipitation of chromium carbide is evidenced (in accordance with the micrographs shown in Figure 1). On the other hand, for nitrocarburized samples, it is visualized the presence of nitride phases (ε-$Fe_{2\text{-}3}N$ and CrN – also confirming the sensitization shown in Figure 1), carbide phases (Fe_3C), and the nitrogen and carbon in solid solution in the martensite lattice (α'_{NC}).

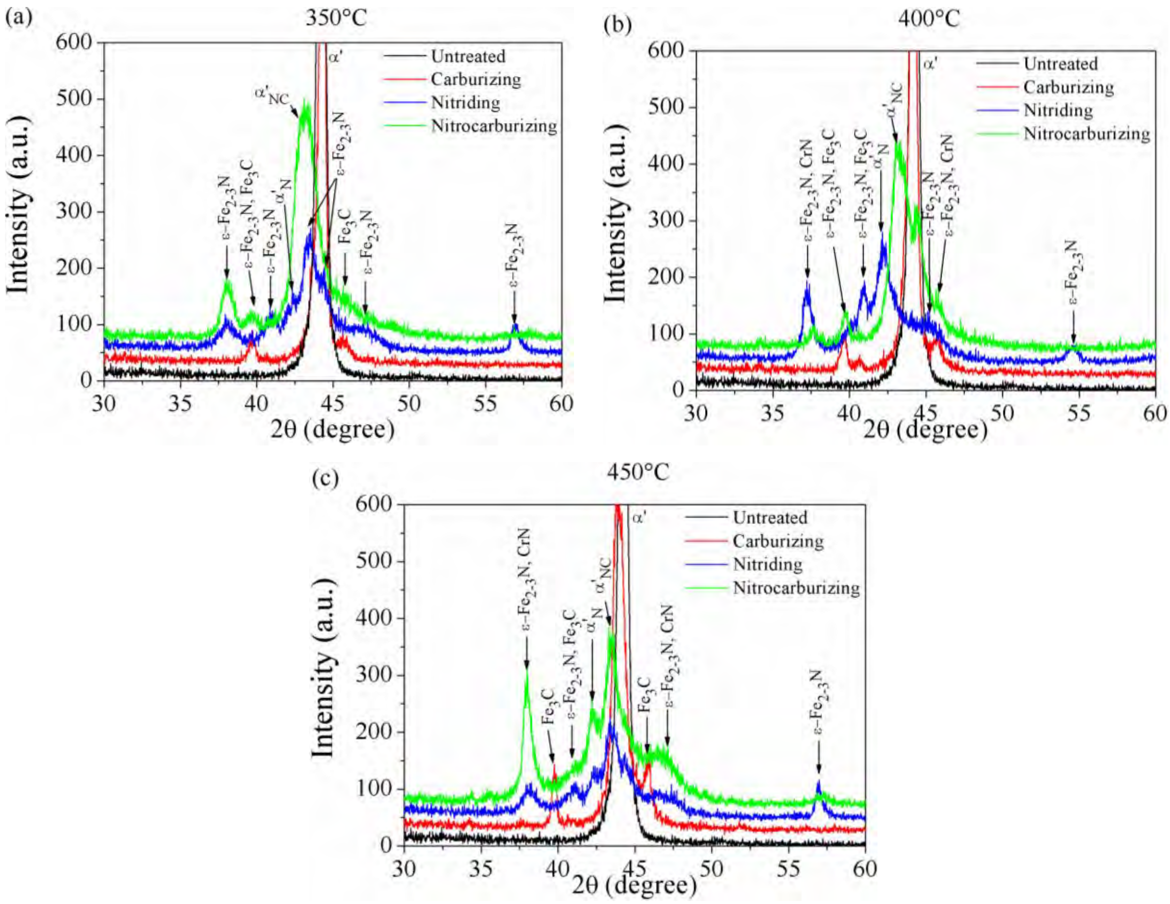

Figure 3. XRD patterns of low-temperature plasma treated AISI 420 martensitic stainless steel. Treatments carried out for 8 h, at a flow rate of 1.67×10^{-6} Nm^3 s^{-1}, applied voltage of 700 V, and pressure of 400 Pa.

ISSN 2176-5480

The evolution of the surface hardness of low-temperature plasma treated AISI 420 martensitic stainless steel for the studied conditions is presented in Figure 4. Measurements were performed on the samples top (surface exposed to the plasma) and bottom (surface non-exposed to the plasma – or substrate bulk). It can be seen that all studied treatments promote an increase of the surface hardness when compared with the bulk hardness. A very slight hardness increase with treatment temperature was verified to carburized samples. By this process, the hardness increases on the order of 1.2, 1.7 and 2.2 times, being that higher increase of hardness is verified for the plasma nitriding and nitrocarburizing processes, which was on the order of 2.2, 3.4 and 3.3 times, and 1.8, 2.4 and 3.5 times, respectively, for treatments performed at 350, 400 and 450ºC. The fact that plasma carburizing, nitriding and nitrocarburizing treatments show distinct hardness increasing rates is related to the different phases and thickness present in the treated layers.

In general, the hardness increase can be attributed to the addition of nitrogen and carbon into solid solution in martensite lattice, allied to the presence of ε-$Fe_{2\text{-}3}N$ and Fe_3C phases, and too, due the treated layer thickness growth, in agreement with that has been presented in Figure 2 and Figure 3. On the other hand, the hardness decrease evidenced at 450°C for the nitriding treatment would be directly related to the strong chromium nitride precipitation, which would reduce the nitrogen content in solid solution and, consequently, the nitrogen-expanded martensite hardness. Finally, a hardness decrease of the sample bottom was verified for all the treated samples, which is a result of the martensite tempering effect. Confronting the sample top and bottom hardness results, it can be noticed that the plasma assisted treatment strengthening effect overcomes the tempering softening one, evidencing the effectiveness of the AISI 420 steel low-temperature plasma assisted treatments studied here.

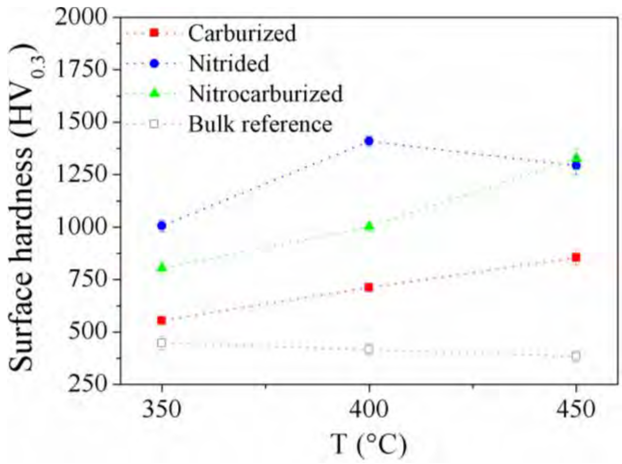

Figure 4. Surface hardness of low-temperature plasma treated AISI 420 martensitic stainless steel. Treatments carried out for 8 h, at a flow rate of 1.67×10^{-6} $Nm^3\ s^{-1}$, applied voltage of 700 V, and pressure of 400 Pa.

Figure 5 shows the comparison between the hardness profile (hardening depth) for the plasma carburized, nitrided and nitrocarburized samples at temperatures of 350 (Fig. 5a), 400 (Fig. 5b), and 450°C (Fig. 5c). By Fig. 5 (a), it can be seen that hardness of 592, 993 and 575 $HV_{0.01}$ at a depth of about 2.5 to 5 µm was verified for samples carburized, nitrided and nitrocarburized at 350°C, respectively. In addition, case depths on the order of 20, 15 and 15 µm, can be also estimated. From Fig. 5 (b), to the samples plasma treated at 400°C, hardness of 738, 1312 and 957 $HV_{0.01}$, and hardening depth of about 40, 25 and 25 µm was verified for carburized, nitrided and nitrocarburized samples, respectively. Finally, Fig. 5(c) shows the comparison of the hardness profiles for samples treated at 450°C employing the different studied techniques. For the plasma carburizing, nitriding and nitrocarburizing treatments, hardness of 872, 1002 and 1157 $HV_{0.01}$ was obtained at distances about 2 to 5 µm from the sample surface, being the case depth about 60 µm for all the carburized, nitrided and nitrocarburized samples.

Figure 6 (a) shows the Ra roughness measurements as a function of treatment temperature for plasma carburized, nitrided and nitrocarburized samples. It can be verified that the untreated samples roughness (~ 0.03 µm) is increased as the treatment temperature is also increased, for all the studied processes. It may be also noted that the roughness are higher for the carburized samples, whereas lower values were obtained for nitrided samples. There are two possible explanations for the fact that the roughness is higher for carburized samples, followed by the nitrocarburized and nitrided ones: a) the higher argon content in the carburizing gas mixture, once argon intensifies the sputtering rate due to its higher atomic weight in relation to the other gas species present in the plasma; and b) due to the higher switched-on time (t_{ON}) applied to the system to keep the treatment temperature. Through Fig. 6(b) it can be seen that for the treatments conducted at temperature of 400°C, the t_{ON} is greater for carburizing, followed by nitrocarburizing, and then by nitriding (to the other treatment temperatures, this same pattern was observed). The higher the t_{ON}, the greater is the effective time of plasma acting, and so the sample bombardment time by the plasma species, resulting in a greater roughness.

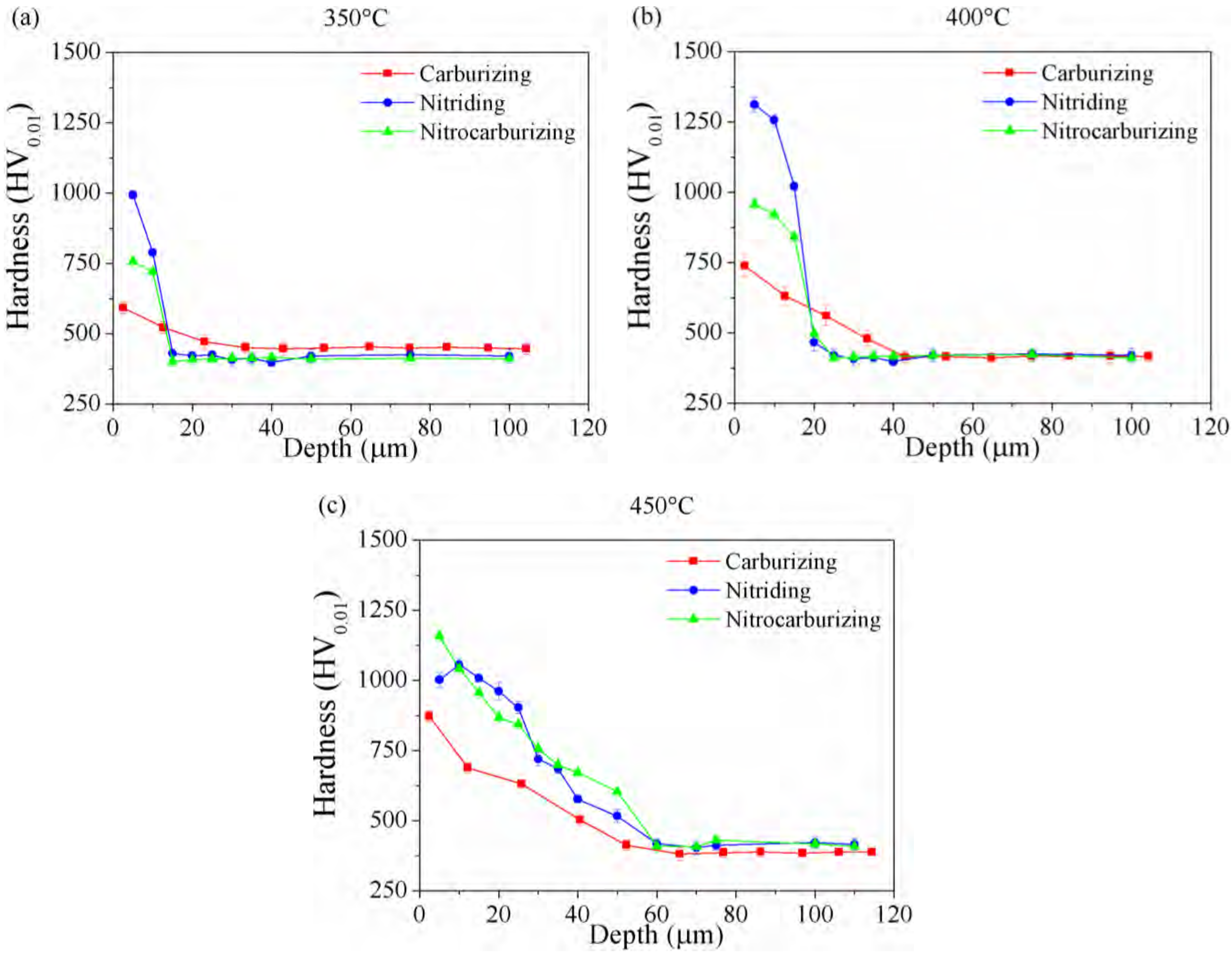

Figure 5. Microhardness profile of low-temperature plasma treated AISI 420 martensitic stainless steel. Treatments carried out at 350, 400 and 450°C for 8 h, at a flow rate of 1.67 × 10^{-6} Nm^3 s^{-1}, applied voltage of 700 V, and pressure of 400 Pa.

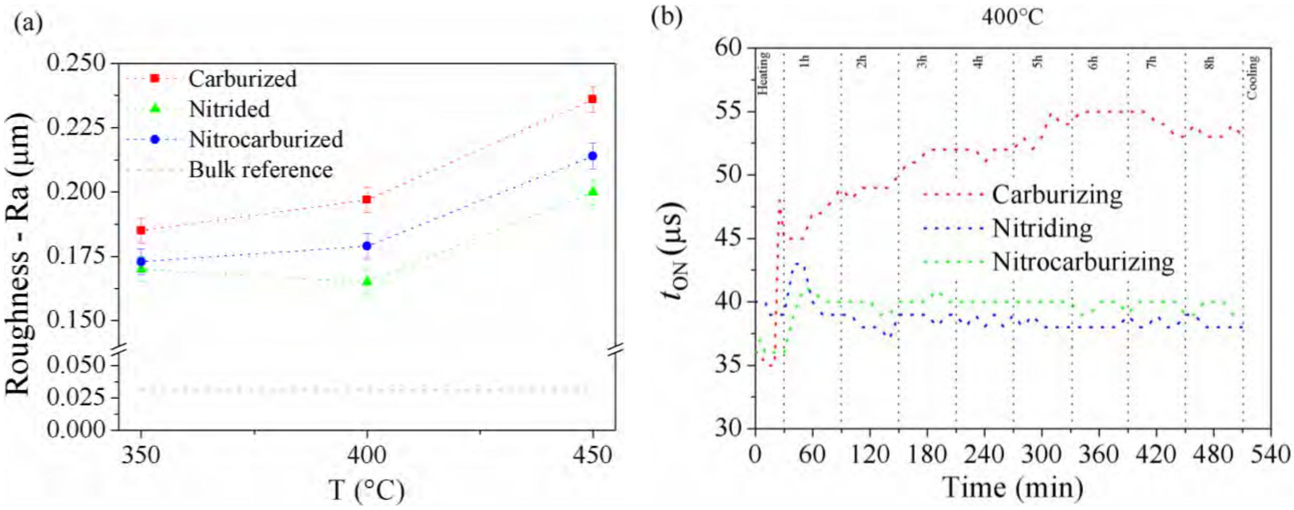

Figure 6. (a) Ra roughness measurements on surface of plasma treated and untreated AISI 420 martensitic stainless steel samples, (b) Switched-on time (t_{ON}) of the pulsed voltage for plasma carburizing, nitriding and nitrocarburizing treatments carried out at a temperature of 400°C. Treatments carried out for 8 h, at a flow rate of 1.67 × 10^{-6} Nm^3 s^{-1}, applied voltage of 700 V, and pressure of 400 Pa.

ISSN 2176-5480

4. CONCLUSION

The effects of the low-temperature (350, 400 and 450°C) and short-time (8 h) DC plasma assisted nitriding, nitrocarburizing and carburizing treatments on the metallurgical characteristics of AISI 420 martensitic stainless steel substrates were investigated in the present work. The main conclusions obtained from the results confrontation can be listed as follows:

- The obtained surface layers are constituted of iron nitrides (for nitriding), carbides (for carburizing), or a mixed structure of nitrides and carbides (for plasma nitrocarburizing). In addition to these constituents, carbon-, nitrogen- and mixed carbon/nitrogen-expanded martensite phase was produced by carburizing (α'_C), nitriding (α'_N) and nitrocarburizing (α'_{NC}), respectively. Furthermore, it has been verified the chromium nitride precipitation occurrence for conditions of 400 and 450°C to the nitrided and nitrocarburized samples;
- The increase of carburizing, nitriding and nitrocarburized temperature leads to a increased layer thickness. Likewise, higher temperatures promote the chromium nitride precipitation in the treated layer, and may result in a surface hardness reduction. Precipitation-free treated layers were obtained to the lowest treatment temperature for all studied conditions;
- The increase of the treatment temperature causes an increase in surface hardness, hardening depth and roughness of the treated samples. The higher hardness is believed to be due to the C/N-expanded martensite phase formation and the occurrence of iron carbide/nitride formation in the treated surface. The hardening depth growing is credited to the greater diffusion coefficient as the temperature is increased. The increased roughness with treatment temperature is explained by the higher switched-on time (t_{ON}) applied to the system to keep the treatment temperature; and, finally,
- The kinetics of the layer growth comprising the carbon and/or nitrogen diffusion changes for the different types of treatments. The estimated activation energy was 29, 136 and 173 $kJmol^{-1}$ for the plasma carburized, nitrided and nitrocarburized samples, respectively.

5. ACKNOWLEDGEMENTS

This work was supported by CNPq, CAPES-COFECUB and Programa Interdisciplinar de Petróleo e Gás Natural da UFPR (PRH24). The authors also wish to express their thanks to the Laboratory of X-ray Optics and Instrumentation – LORXI, from the Universidade Federal do Paraná (UFPR) by the use of the X-ray diffraction equipment.

6. RESPONSIBILITY NOTICE

The authors are the only responsible for the printed material included in this paper.

REFERENCES

[1] C. X. Li, T. Bell. A comparative study of low temperature plasma nitriding, carburising and nitrocarburising of AISI 410 martensitic stainless steel. Materials Science and Technology, v. 23(3), pp. 355-361, 2007.
[2] Z.L. Zhang, T. Bell. Structure and corrosion resistance of plasma nitride stainless steel. Surface Engineering, v. 1, pp. 131–136, 1985.
[3] Y. Sun, T. Bell, G. Wood. Wear behaviour of plasma-nitrided martensitic stainless steel. Wear, v. 178, pp. 131-138, 1994.
[4] C.X. Li, T. Bell. LI, C. X., BELL, T. Corrosion properties of plasma nitrided AISI 410 martensitic stainless steel in 3.5% NaCl and 1% HCl aqueous solutions. Corrosion Science, v. 48, p. 2036-2049, 2006.
[5] Y. Sun, T. Bell. Sliding wear characteristics of low temperature plasma nitrided 316 austenitic stainless steel. Wear, v. 218, pp. 34-42, 1998.
[6] E. Menthe, K.-T. Rie, J.W. Schultze, S. Simson. Structure and properties of plasma-nitrided stainless steel. Surface & Coatings Technology, v. 74–75, pp. 412-416, 1995.
[7] E. Menthe, A. Bulak, J. Olfe, A. Zimmermann, K.-T. Rie. Improvement of the mechanical properties of austenitic stainless steel after plasma nitriding Surface & Coatings Technology, v. 133–134 pp. 259-263, 2000.
[8] F. Borgioli, A. Fossati, E. Galvanetto, T. Bacci. Glow-discharge nitriding of AISI 316L austenitic stainless steel: influence of treatment temperature. Surface & Coatings Technology, v. 200, pp. 2474– 2480, 2005.
[9] S. K. Kim, J. S. Yoo, J. M. Priest, M. P. Fewell. Characteristics of martensitic stainless steel nitrided in a low-pressure RF plasma. Surface & Coating Technology, v. 163-164, pp. 380-385, 2003.

[10] C.J. Scheuer, R.P. Cardoso, M. Mafra, S.F. Brunatto. AISI 420 martensitic stainless steel low-temperature plasma assisted carburizing kinetics. Surface Coating & Technology, v. 24, pp. 30-37, 2013.
[11] P. Corengia, G. Ybarra, C. Moina, A. Cabo, E. Broitman, Microstructure and corrosion behaviour of DC-pulsed plasma nitride AISI 410 martensitic stainless steel. Surface & Coating Technology, v. 187, pp. 63-69, 2004.
[12] P. Corengia, F. Walther, G. Ybarra, S. Sommadossi, R. Corbari, E. Broitman. Friction and rolling–sliding wear of DC-pulsed plasma nitrided AISI 410 martensitic stainless steel. Wear, v. 260, pp. 479–485, 2006.
[13] C.X. Xi, D.X. Liu, D. Han. Improvement of mechanical properties of Martensitic stainless steel by plasma Nitriding at low temperature. Acta Metallurgica Sinica (English Letters), v. 21, p. 21–29, 2008.
[14] C.X. Xi, D.X. Liu, D. Han. Improvement of corrosion and wear resistances of AISI 420 martensitic stainless steel using plasma nitriding at low temperature. Surface & Coatings Technology, v. 202, pp. 2577–2583, 2008.
[15] C.X. Xi, D.X. Liu, D. Han. Improvement of corrosion and wear resistances of AISI 420 martensitic stainless steel using plasma nitriding at low temperature. Surface & Coatings Technology, v. 202, p. 2577–2583, 2008.
[16] L.A. Espitia, L. Varela, C.E. Pinedo, A.P. Tschiptschin. Cavitation erosion resistance of low temperature plasma nitrided martensitic stainless steel. Wear. in press (accessible in: http://www.sciencedirect.com/science/article/pii/S0043164812004577, DOI information: 10.1016/j.wear.2012.12.029.
[17] F.A.P. Fernandes, G.E. Totten, J. Gallego, L.C. Casteletti. Plasma nitriding and nitrocarburising of a supermartensitic stainless steel. International Heat Treatment and Surface Engineering, v. 6(1), pp. 24-27, 2012.
[18] R.L. Liu, M.F. Yan, Improvement of wear and corrosion resistances of 17–4PH stainless steel by plasma nitrocarburizing. Materials & Design. v. 31, pp. 2355–2359, 2010.
[19] M.F. Yan, R.L. Liu, Influence of process time on microstructure and properties of 17-4PH steel plasma nitrocarburized with rare earths addition at low temperature. Applied Surface Science, v. 256, pp. 6065–6071, 2010.
[20] M.F. Yan, R.L. Liu, D.L. Wu, Improving the mechanical properties of 17-4PH stainless steel by low temperature plasma surface treatment. Materials & Design. v. 31, pp. 2270–2273, 2010.
[21] R.L. Liu, M.F. Yan, Y.Q. Wu, C.Z. Zhao, Microstructure and properties of 17-4PH steel plasma nitrocarburized with a carrier gas containing rare earth elements. Materials Characterization, v. 61 pp. 19-24, 2010.
[22] C.J. Scheuer, R.P. Cardoso, R. Pereira, M. Mafra, S.F. Brunatto. Low temperature plasma carburizing of martensitic stainless steel. Materials Science and Engineering A, v. 539, pp. 369–372, 2012.
[23] C.J. Scheuer, R.P. Cardoso, F.I. Zanetti, T. Amaral, S.F. Brunatto. Low-temperature plasma carburizing of AISI 420 martensitic stainless steel: Influence of gas mixture and gas flow rate. Surface & Coatings Technology, v. 206, pp. 5085–5090, 2012.
[24] C.J. Scheuer, A.D. dos Anjos, R.P. Cardoso, S.F. Brunatto. Estudo morfológico e cinético da nitrocarbonetação a baixa temperatura assistida por plasma do aço inoxidável martensítico AISI 420. 7° Congresso Brasileiro de Engenharia de Fabricação (7° COBEF), 15th to 19th april, Pinedo/Itatiaia, Rio de Janeiro, Brazil, 2013.
[25] T.F. Amaral, F.I. Zanetti, C.J. Scheuer, S.F. Brunatto, R.P. Cardoso. Influence of previous heat treatment on the AISI 420 steel low temperature nitriding kinetics. Book of abstracts of the X Brazilian MRS Meeting, Gramado, Brazil, 2011.
[26] C. E. Pinedo, W. A. Monteiro. On the kinetics of plasma nitriding a martensitic stainless steel type AISI 420. Surface and Coatings Technology, v. 179, pp. 119–123, 2004.